Composites Science and Technology 245 (2024) 110339

Contents lists available at ScienceDirect

Composites Science and Technology

journal homepage: www.elsevier.com/locate/compscitech

Manufacture and characterisation of a structural supercapacitor demonstrator

Sang Nguyen [a,*], David B. Anthony [a,b], Tomas Katafiasz [a], Guocheng Qi [a,e], Seyedalireza Razavi [a], Evgeny Senokos [b], Emile S. Greenhalgh [a], Milo S.P. Shaffer [b], Anthony R.J. Kucernak [b], Peter Linde [c,d]

[a] The Composite Centre, Department of Aeronautics, Imperial College London, UK
[b] Department of Chemistry, Department of Materials, Imperial College London, UK
[c] Department of Industrial and Materials Science, Chalmers University of Technology, Gothenburg, Sweden
[d] German Aerospace Center (DLR), Bonn, Germany
[e] Institute of Engineering Mechanics, Beijing Jiaotong University, Beijing, 100044, People's Republic of China

ARTICLE INFO

Keywords:
A. Multifunctional composites
A. Structural composites
B. Electrical properties
Demonstrator

ABSTRACT

Structural power composites, a class of multifunctional materials, may facilitate lightweighting and accelerate widespread electrification of sustainable transportation. In the example considered in this paper, structural power composite fuselage components could provide power to open aircraft doors in an emergency and thus reduce or eliminate the mass and volume needed for supercapacitors currently mounted on the doors. To demonstrate this concept, an 80 cm long multifunctional composite C-section beam was designed and manufactured, which powered the opening and closing of a desktop-scale composite aircraft door. Twelve structural supercapacitor cells were made, each 30 cm × 15 cm × 0.5 mm, and two stacks of four cells were integrated into the web of the beam by interleaving and encasing them with low-temperature-cure woven carbon fibre/epoxy prepreg. This article culminates by considering the engineering challenges that need to be addressed to realise structural power composite components, particularly in an aerospace context.

1. Introduction

1.1. Background

Structural power composites (SPCs) [1] can significantly reduce the parasitic mass associated with conventional energy storage devices and facilitate widespread electrification in sustainable transportation [2–4]. These emerging multifunctional materials store and deliver electrical energy as well as support mechanical loads. Structural supercapacitors [5] have lower energy densities but higher power densities than those of structural batteries [6], with potential applications for electrical load levelling, buffering and high power delivery. Despite growing interest in structural batteries and structural supercapacitors, much of the research to date has focused on developing the multifunctional constituents (i.e., the electrodes/reinforcements and/or the structural electrolyte) rather than manufacture, scale-up, assembly of multiple cells and demonstration [7] (Fig. 1): the focus of this study is a multicell structural supercapacitor demonstrator for an aerospace application.

Due to their greater maturity and reduced complexity, more large-scale (i.e. multicell) demonstrators have been reported for structural supercapacitors than for structural batteries [8]. Examples of such previous demonstrators and their characteristics are presented in Fig. 1 and Table 1. The associated electrical performance requirements have been fairly modest: representative of low power and energy applications such as lighting [9,10]. Structural components for demonstration have been selected to be easily identifiable to all target groups and not necessarily on the basis of optimal system weight saving considerations.

Other considerations for structural component selection have included the ease of access for replacement, similar stiffness demands to those achievable by the SPCs developed in the corresponding research projects and space to allow for thicker laminates and additional wiring. In all of the demonstrators developed to date, the approach has primarily involved direct replacement of the existing structural components. The geometries have been kept the same as the original parts and

* Corresponding author.
E-mail address: snguyen@ic.ac.uk (S. Nguyen).

https://doi.org/10.1016/j.compscitech.2023.110339
Received 6 December 2022; Received in revised form 31 August 2023; Accepted 2 November 2023
Available online 11 November 2023

only the thickness of the component differed from that of the originals. In some cases, finite element modelling has been carried out to design the multifunctional component so as to meet the structural requirements [9,10].

Several challenges arise when manufacturing large scale multifunctional demonstrator components that are not encountered when manufacturing single-cell lab-scale devices [12]. The key issues include (i) current collection, (ii) multicell assembly, (iii) reproducible manufacturing and (iv) moisture-free manufacture/encapsulation. (i) The relatively low electrical conductivity of carbon fibres as compared to that of metals can lead to large power losses due to high equivalent series resistances (ESR) for thin devices with large areas [13]. (ii) Scale-up to a realistic component designed for application, requires using multiple cells to meet the desired operating voltages, presenting new challenges in physical integration and electrochemical cell balancing. Most power sources consist of stacks or cylindrical configurations of small cells [2]. However, efficient structural configurations rely on continuous load paths throughout the structure. Hence, to optimise mechanical and electrochemical efficacy, the packaging arrangement for multiple SPC cells requires greater consideration than for a single cell. (iii) For multicell structural power components, the manufacturing process presents more challenges than that of a conventional composite or electrochemical device. The relatively small-scale fabrication of SPCs to date have shown only modest cell to cell reproducibility [14]. Variability in the cell capacitance and equivalent series resistance (ESR) can lead to an uneven voltage distribution in multicell stacks, suitable for application, leading to lost capacity. The pressure applied during manufacture and electrochemical characterisation of a cell can have a critical influence on the contact resistances, particularly those between the electrodes and current collectors. Furthermore, thin constituents, such as the separator, or spread tow fabrics, can be difficult to handle manually as large sheets without introducing wrinkles or other such defects. (iv) Manufacture in a moisture-free environment to permit high voltage operation without electrochemical degradation requires fabrication in a dry box or dry room. Very often, in a laboratory setting, researchers default to using a glove box widely used for battery manufacture. However, the requirement for a controlled atmosphere can introduce difficulties associated with the size of the glove box airlock, reduced manual dexterity and being able to use conventional composite manufacturing equipment. Overall, the literature contains significant gaps in scale up and manufacture of multicell structural supercapacitor demonstrators, full characterisation of the mechanical and electrochemical properties and the variability in such properties between nominally-identical cells.

Table 1
Structural supercapacitor technology demonstrators [9,10].

Structural component	Electrical system powered	Cells	Voltage (V)
Small scale car body shell [9]	LED lights	1	3
Small scale Volvo car roof [9]	LED lights	2	6
Aircraft electronics box casing [11]	Power spike buffer	15	30
Volvo S80 boot lid [9,10]	External rear lighting	16	12

1.2. Aims

This study aimed to manufacture a structural supercapacitor technology demonstrator to (a) aid researchers, stakeholders and the general public in grasping the concept of energy-storing structural materials; (b) elevate the technology readiness level of SPCs and (c) gain an improved understanding of the practical and engineering issues associated with scaling up from small lab-scale single-cell devices to larger multicell structural components. The structural and electrical components selected were representative of an Airbus A380-800 fuselage C-section beam (Fig. 2a) and a bank of conventional supercapacitors (Fig. 2b)

Fig. 1. (a,b) Desktop scale (approximately 30 cm long) structural supercapacitor composite demonstrators in the form of automotive exterior panels able to power lights [9], (c–f) Full scale Volvo S80 boot lid demonstrator with integrated structural supercapacitors to power external lights [9].

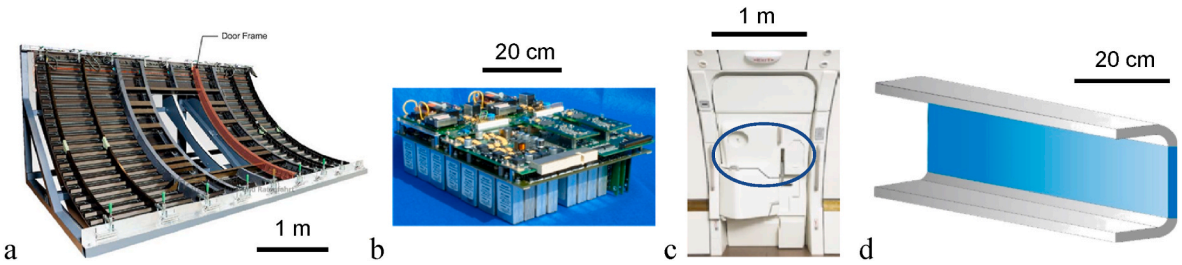

Fig. 2. (a) Location of the curved fuselage beam shown in red [15,16], (b) conventional supercapacitor bank and circuit board [17], (c) passenger door with the location of the supercapacitor bank circled [17], (d) proposed multifunctional web of the C-beam [17].

located on the aircraft cabin door (Fig. 2c). These supercapacitors provide a backup power source, generating a torque to open the door in an emergency.

Only a short, straight section (80 cm long), rather than a full length curved C-beam, was manufactured as a demonstrator. The size of the fuselage section supporting the door was scaled down to approximately 40 cm wide and 30 cm high, both to moderate power requirements and provide a useful, portable system. The aspiration was to make a multifunctional aerostructure, directly related to aircraft design (Fig. 2d): in the current embodiment, the representative element stores energy in the web region (blue) where the structural requirements are less demanding. The potential mass and volume savings if SPCs were adopted to power all sixteen passenger doors on the aircraft would be approximately equal to the mass (67 kg) and volume (0.21 m^3) of sixteen supercapacitor banks. Both of these benefits are conditional on the SPC being able to completely fulfil both the structural and electrical requirements provided by the existing beams and conventional supercapacitor banks, respectively, without significant changes in mass or volume compared to the conventional structural beams.

2. Experimental details

2.1. Device manufacture

Twelve plies of Textreme 43 PW HS40 12 K plain weave spread tow carbon fibre fabrics (43 gsm, Oxeon AB, Sweden) reinforced with carbon aerogel (CF-CAG) [18], of dimensions 30 cm × 22 cm × 0.2 mm, were manufactured using the method reported in Ref. [19] (Fig. 3a). Thin plies were used to enable stacking of sufficient cells to achieve the required operating voltage within the thickness of the C-beam. These plies were cut in half lengthwise and trimmed to 28 cm × 11 cm. Strips of 28 cm × 1 cm Wurth Electronik 3013310A conductive adhesive Al tapes from RS Components were attached to the electrodes with 1 cm transverse spacing between the lengthwise tapes. Tapes that protruded 10 cm outside the electrode area were folded back and self-adhered to leave 5 cm long external connectors. Patterned epoxy droplets were applied to the non-binder side of the CF-CAG plies with one drop at the centre of each 2 cm × 2 cm unit cell in the weave (Fig. 3b). This method of bonding in discrete locations was similar to the resin plugs [11] or polymer rivets [20] concepts in other studies, with the main difference being that, in this study, no holes were introduced in the electrodes, so the load paths through the reinforcements were continuous. This pragmatic method was used instead of the prepregged bicontinuous structural electrolyte approach because the structural electrolyte had been shown to form a heterogeneous microstructure in the presence of fibrous electrodes, reducing electrochemical performance [19]. The epoxy was the same as that used in Ref. [19]: bisphenol A diglycidyl ether (DGEBA) mixed with isophorondiamine (IPDA) hardener, both supplied by Sigma Aldrich mixed in a 4:1 ratio of DGEBA to IPDA by weight.

Each pair of electrodes was separated by a Freudenberg FS 3002–23 polyester-ceramic separator ply (30 cm × 13 cm × 23 μm) (Fig. 3c): to ensure consistent manufacturing conditions each pair of electrodes came from the same CF-CAG ply (Fig. 3d). Each device was then cured at 120 °C under 1.3 kPa pressure for 2 h in a Memmert UN55plus oven.

A 71 μm thick aluminized moisture-proof pouch (Desco Industries Inc, SCS static shielding bag, 1000 series) was sealed around the protruding connectors (Fig. 3e) using Pi-Kem holt melt sealing tape (Fig. 3f) heated to 160 °C for 5 s using a FlowerW FR900 heat sealer (Fig. 3g–i). Each pouch cell was infused with 9 ml 1-ethyl-3-methylimidazolium bis (trifluoromethylsulfonyl)imide (EMIM-TFSI, >98 %, Sigma Aldrich) ionic liquid electrolyte (Fig. 3j) under vacuum using a Buffalo CD969 Light Duty Chamber Vacuum Pack Machine to impregnate the pores (Fig. 3k). The manufacture was divided into three batches of four cells made together on the same date. The average cell thickness including the encapsulation was 0.5 mm. To check as to whether any moisture uptake had occurred, the mass of each cell was measured after assembly and approximately three months later.

2.2. Device characterisation

The electrochemical characterisation was carried out using electrochemical impedance spectroscopy (EIS) and galvanostatic charge-discharge (GCD) tests at different current densities. These tests used a four-channel Biologic VSP-3e potentiostat and the methods detailed in Ref. [19]. EIS was performed at a bias voltage of 0 V with a potential amplitude of 10 mV and a frequency range of 100 mHz to 20 kHz. For GCD, the current density used for reporting the results was 1 mA/cm^2, selected to match the current density at which the demonstrator was expected to operate when opening and closing the door. The laboratory temperature and relative humidity (RH) when performing the electrochemical tests were 23 ± 2 °C, and 40 ± 10 % RH, respectively. The discharge specific capacitance was measured after at least five cycles to ensure that the measured capacitance had stabilised, and after at least 100 cycles to characterise cycling performance. The ESR was calculated from the high frequency intercept with the x-axis in the EIS plots. During electrochemical testing, the cells were placed on a compliant Pacopad (Pacothane Technologies #5500) sheet to uniformly distribute the load, and a constant pressure was applied to the cells by covering them with a second Pacopad sheet, followed by a 30 cm × 30 cm × 4 mm (1 kg) aluminium plate. A modest through-thickness pressure was applied for electrochemical testing using several 5 kg and/or 2 kg calibrated weights to minimise internal contact resistances. The default weight of 21 kg corresponded to a pressure of 6.7 kPa over the entire electrode area (Fig. 4a). This pressure was chosen because sufficient pressure was needed to promote good electrical contact between the interfaces in the cells whilst being low enough to reduce charge leakage observed at higher pressures.

Further tests were also performed without the Pacopad to investigate the influence of the applied pressure transmitted directly via the aluminium plates up to a maximum of 22.3 kPa (Fig. 4b).

2.3. Demonstrator manufacture

Following electrochemical characterisation, eight of the cells

Fig. 3. (a) Spread tow CF-CAG plies, (b) patterning of epoxy droplets, (c) lay up of electrodes sandwiching the separator, (d) assembled cells without encapsulation, (e) placement of cell into encapsulation, (f) insertion of hot melt tape around connectors, (g) heat sealing around connectors, (h) encapsulation sealed around connectors (i) heat sealing of edges of encapsulation, (j) insertion of electrolyte, (k) vacuum sealing.

(Fig. 5a, Fig. 6a) were selected for integration in the beam. Cells 1, 2 and 3 were omitted because they had relatively high ESRs compared to those of the other cells, whilst cell 12 was omitted because it had the lowest measured specific capacitance.

The cell connectors were extended by attaching additional lengths of aluminium tape with conductive adhesive such that the connectors would protrude from the ends of the beam. These extended connectors were insulated using polyester tape leaving 1 cm uncovered for electrical connections. Plies of woven SHD Composites LTC102 low temperature cure epoxy tooling prepreg (T300 HS fibres, 0.25 mm ply thickness) were cut such that they would closely surround the cells when placed in the web section of the beam (Fig. 5b). Using the same prepreg,

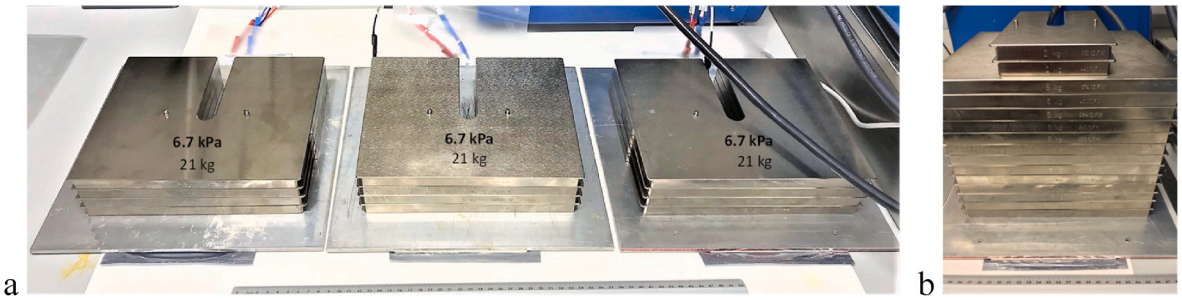

Fig. 4. Arrangement for electrochemical characterisation of (a) multiple cells with 6.7 kPa pressure, (b) a single cell with 22.3 kPa pressure.

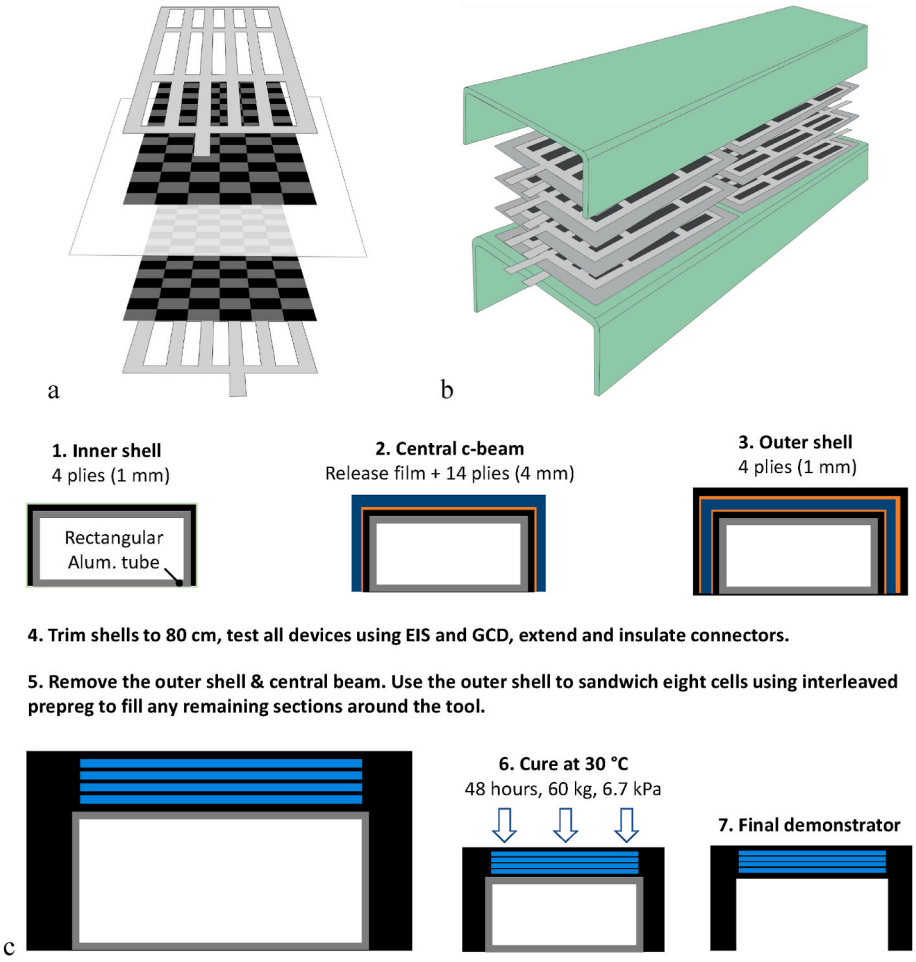

Fig. 5. (a) Schematic of plies in one cell, (b) arrangement of the cells in the C-beam, (c) manufacturing procedure for integration of structural supercapacitors into the C-beam.

a 1 mm thick (four plies) inner shell was made by laying up on the outside of a 100 cm long × 20 cm wide (externally) × 10 cm high (externally) × 4 mm thick rectangular aluminium tube section (Figs. 5c and 6c) and cured using a heated vacuum table at 70 °C for 8 h. After covering the inner shell with release film, a 4 mm thick central structural C-beam was manufactured over the inner shell (Figs. 5c and 6c). This central beam was used to maintain the correct spacing between the inner and outer shells and was not included in the final demonstrator. By using the outer surface of the central C-beam covered with release film as a tool, a 1 mm thick outer shell was made (Figs. 5c and 6c). To promote adhesion, the surfaces of both the inner and outer shells that would subsequently contact prepreg were sanded using MetPrep P320 metallographic abrasive paper. Two stacks of four encapsulated cells were then assembled on the inner skin taking care to ensure cell alignment (Fig. 5b).

Additional low temperature cure prepreg was laid up surrounding the cells and in the cap regions with two plies to achieve approximately the same thickness as the cells (0.5 mm). Two plies of 85 cm × 40 cm prepreg were interleaved between the stacks of cells. The stacks were then sandwiched between the two precured shells, with electrical connectors extending from each end of the beam. The outer shell was placed over the assembly containing the stacks followed by curing in the heated vacuum table. The aluminium tooling was used to support the beam, with 60 kg distributed weight (6.7 kPa) at 30 °C for 48 h applied to the outer face of the web (Figs. 5c and 6d).

The final multifunctional beam (Fig. 6e and f) was trimmed with a

Fig. 6. (a) Four of the twelve structural supercapacitor composite cells, (b) cells integrated into the beam, (c) inner, central and outer structural shells, (d) consolidation and curing of the SPC beam, (e) inner surface of the SPC beam, (f) outer surface of the SPC beam, (g) computer aided design model of scaled fuselage door assembly and SPC beam, (h) inside and (i) outside of fuselage door assembly. For an indication of scale, the cells are 30 cm long, the beam is 80 cm long and the fuselage is 40 cm wide.

dry diamond-tipped circular saw, taking care to avoid damage to the electrical connectors. Each cell was electrochemically characterised using the methods described in Section 2.2.

A computer aided design (CAD) model (Fig. 6g) of an aircraft fuselage and passenger door assembly (40 cm wide × 33 cm high × 13 cm deep with the door closed) was generated using Pro/Engineer and manufactured (Fig. 6h and i). The majority of the parts were 3D printed from ABS using a Stratasys Fortus 400mc 3D Printing System. The fuselage, door and floor panel were made from the same low temperature cure prepreg as that used for the C-beam structural plies. A 6 V DC Parallax Standard Servo #900-00005 motor from RS Components controlled by a Sparkfun WIG 13118 servo trigger board from Farnell was used to drive the door mechanism with a 3 s actuation time. Power for the door was supplied by four of the cells at one end of the beam connected in series such that each cell was charged to around 1.5 V.

3. Results and discussion

This section presents results from characterisation of the devices before and after integration into the C-beam. The main issue encountered during the fabrication process was that various structural encapsulation materials were investigated but were found to either not transfer load to the electrodes in the presence of the electrolyte or chemically interacted with the electrolyte, leading to electrochemical performance degradation. Therefore, conventional aluminized polymer heat-sealable pouches, as used for battery pouch cells, were used as the encapsulation material.

3.1. Device description

The average mass and volume of a single packaged cell were 32.84 ± 1.02 g and 20 cm^3, respectively. The average total mass increase over three months (16/8/21 to 11/11/21) was around 1 %, which was attributed to gradual moisture ingress. Breakdowns of the masses and thicknesses of the constituents for a conventional supercapacitor were obtained from disassembling a cylindrical Maxwell 150 F supercapacitor of similar mass (32 g) and volume (25 cm^3) [21], and measured for the structural supercapacitor cells in the demonstrator (Fig. 7).

The electrolyte and epoxy were deemed to have negligible contribution to the overall cell thickness, since they were incorporated in the pores of the electrodes and separator (i.e., the thin epoxy bond-line was excluded). For both conventional and structural supercapacitors, the current collection and encapsulation together occupied over half the cell mass and volume. This breakdown suggests that substantial improvements in mass and volume savings could be achieved by investigating lighter and thinner alternatives to current collection and encapsulation strategies. To improve overall gravimetric and volumetric performance, development of current collection and encapsulation solutions are perhaps as important as research into optimising the electrodes, structural electrolyte and separators, although the latter constituents have tended to be the main subject of research to date [5]. For the whole C-beam component, the relative proportion of encapsulation mass and

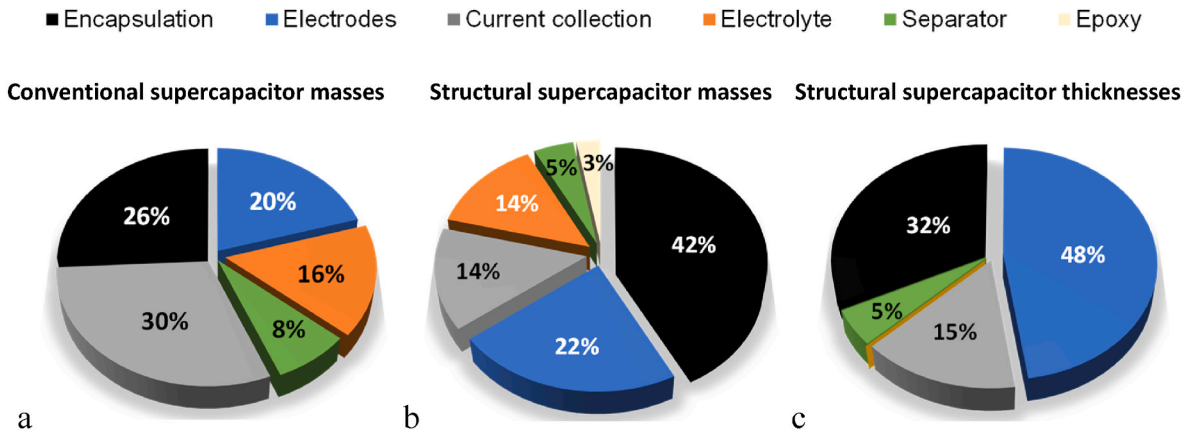

Fig. 7. Relative proportion by mass of constituents in single cells of a (a) conventional supercapacitor and (b) structural supercapacitor as used in the demonstrator. (c) Relative proportion by thickness of constituents in single structural supercapacitor cells.

volume could have been reduced by packaging all the cells together with a single encapsulation pouch. For this demonstrator, in case any cells became faulty, each cell was encapsulated separately to permit electrical isolation by excluding the cell from the electrical circuit.

3.2. Device characterisation

The pressure applied during electrochemical characterisation was critical to performance. As the pressure increased, the device ESR tended to fall, plateauing when approximately 22 kPa pressure was applied (Fig. 8a). At the maximum pressure, the cell could only charge to ca. 1.0 V as compared to 1.8 V at the minimum pressure (Fig. 8b).

This reduction in maximum voltage was attributed to a reduced separation distance and greater charge leakage between the electrodes [14]. The influence of pressure on electrochemical performance may be an important consideration if SPCs are used in structural components that experience large pressure variations during service. However, improved current collector and encapsulation design is likely to reduce this sensitivity.

To measure the inherent variability associated with the electrochemical testing, eight repeated tests were performed on the same cell under nominally identical test conditions without removing the pressure between tests (Fig. 9). The general shape and gradients of the EIS responses were very similar, but the ESR had a variation of ±16 Ω cm^2 (±13 %). A maximum discharge energy of 11.3 mWh was measured for a single cell under 1.3 kPa pressure when charged up to 2.7 V (Fig. 10). The specific energies normalised by the encapsulated device mass including excess ionic liquid (32.36 g), excluding excess ionic liquid (18.53 g) and excluding both excess ionic liquid and encapsulation (9.77 g) are shown in Fig. 11a. Excess ionic liquid (13.83 g) was defined as the amount in addition to that needed (2.63 g) to fill the pores of the electrodes and separator.

The highest specific energies and maximum specific powers (Fig. 11) provided upper bound estimates for the performance if good electrical contact were to be achieved.

This performance could be achieved by maintaining a suitable pressure that avoided a high leakage current and if the ionic liquid quantity and combined encapsulation of all of the cells could be optimised to minimise parasitic mass. At 2.7 V, as reached in Fig. 10, the theoretical maximum specific energy was 1.28 Wh/kg. Since the maximum measured specific energy was only 0.35 Wh/kg, it was apparent that only between a quarter and a third of the energy stored during charging was recovered during discharge (Fig. 10). This low

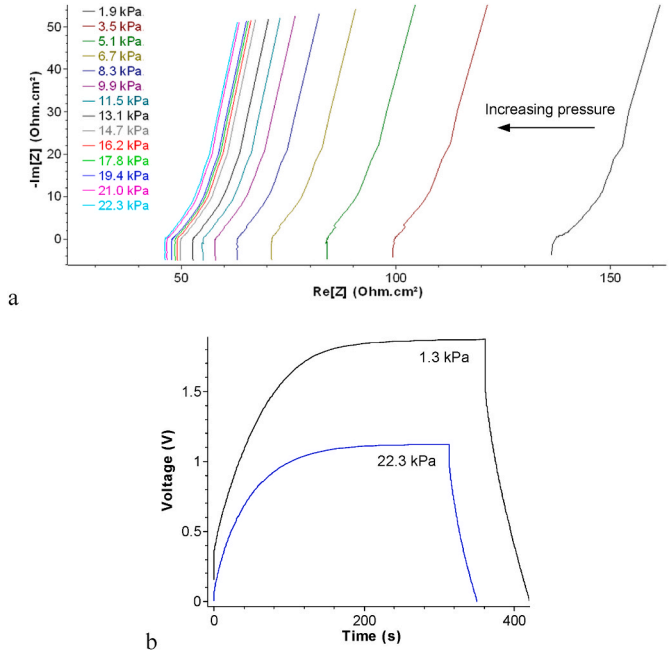

Fig. 8. Effect of pressure on (a) impedance pre-integration, cell 3, tested on 18/8/21, (b) galvanostatic charge-discharge, 1 mA/cm^2, cell 3, tested on 3/8/21 and 18/8/21.

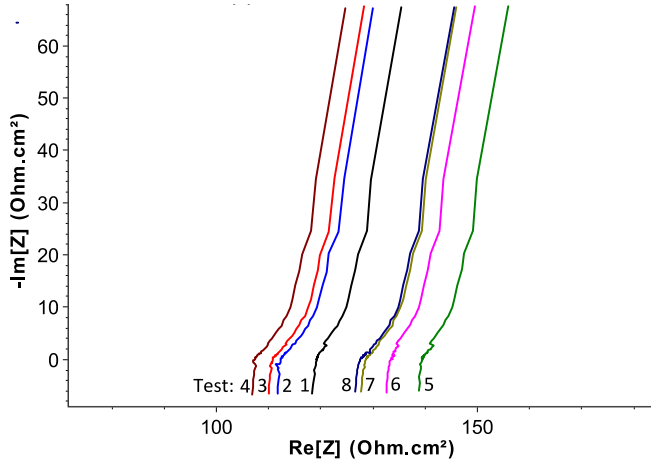

Fig. 9. Inherent variability in impedance, 6.7 kPa, cell 5, tested on 20/8/21, Test 1 = 1st test, etc.

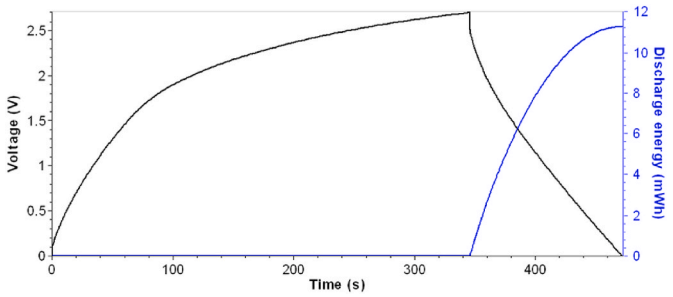

Fig. 10. Voltage and discharge energy against time, 1.3 kPa, cell 11, 1 mA/cm^2, tested on 18/8/21.

energy efficiency may have been due to a high leakage current, particularly above 1.8 V, as suggested by the reduction in gradient of the voltage-time curve during charging (Fig. 10). Alternatively, parasitic water electrolysis may have led to the low energy efficiency.

The cells manufactured earlier generally had higher specific capacitance than those in the later batches (Fig. 12). This observation may have resulted from better permeation of ionic liquid throughout the cells manufactured earlier. To improve reproducibility of the properties between cells, further work is needed to automate the manufacturing processes, for example by using a robotic adhesive dispensing system to apply the patterned epoxy droplets. After approximately four months, the average specific capacitance had dropped to 0.28 mF/g, but this reduction was within the measurement variations.

3.3. Demonstrator characterisation and evaluation

The completed SPC C-beam demonstrator weighed 2.7 kg and had a web thickness of 7 mm. The beam was 80 cm long, 20 cm wide in the web region (externally) and 10 cm deep in the cap regions (externally). A purely structural C-beam using the same number of prepreg plies weighed 2.7 kg and had a thickness of 6 mm. Soon after manufacturing the cells (pre-integration), charging three or four of the structural supercapacitor cells connected in series to 6 V for 10 s could power the door mechanism (Fig. 13) to open and close three times.

Post-integration, a charge time of 30 s was needed to open and close the door three times, which was attributed mainly to the higher ESR resulting from a lower pressure maintained on the cells within the C-beam. A video showing the demonstrator operation is accessible via the link in Appendix A. The total energy stored based on average values measured at 1 mA/cm^2 up to 1.5 V was approximately 10 mWh and the average power output when opening the door mechanism was 0.5 W. The total mass of the cells represented less than 10 % of the total beam weight. Therefore, significantly more energy could be stored by having a greater proportion of structural supercapacitor composite mass. Additional mechanical evaluation would be needed in further work to compare the performances of the multifunctional and the monofunctional systems.

Some energy storage functionality has been introduced without changing the weight of the beam. Hence the weight of the conventional supercapacitors that would otherwise operate the door could be considered as the weight saving, provided that the SPC beam meets the mechanical performance requirements of the application. However, any mechanical performance reductions would also need to be included in a more accurate weight saving analysis. In the current form, the SPC beam would have both reduced stiffness and strength relative to the original beam for two main reasons. Firstly, a suitable encapsulation material that transfers load between the structural supercapacitor cells and the surrounding CFRP has not been implemented. Such a load-transferring encapsulation material is the topic of ongoing research. Secondly, the structural supercapacitors themselves have reduced stiffness and strength relative to CFRP [19]. To minimise the impact on structural performance, the structural supercapacitors were integrated into the web region where the structural performance is less critical than that for the caps. This article highlights the scale-up challenges and lessons learnt from manufacturing a demonstrator; significant development work is still needed to manifest weight savings compared to using a combination of conventional composite manufacturing and supercapacitor technologies. The structural electrolyte manufacturing process needs to be scaled up and developed such that the final microstructure can be better controlled.

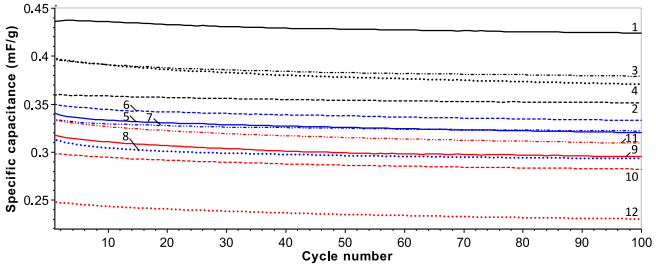

Fig. 12. Specific capacitance at 1 mA/cm^2 normalised by the total mass of the encapsulated cell, pre-integration, 1.3 kPa. The numbers refer to the cell numbers. The colours refer to the batch number: batch 1 (tested 16 days after manufacture), batch 2 (tested 3 days after manufacture), batch 3 (tested on same day as manufacture).

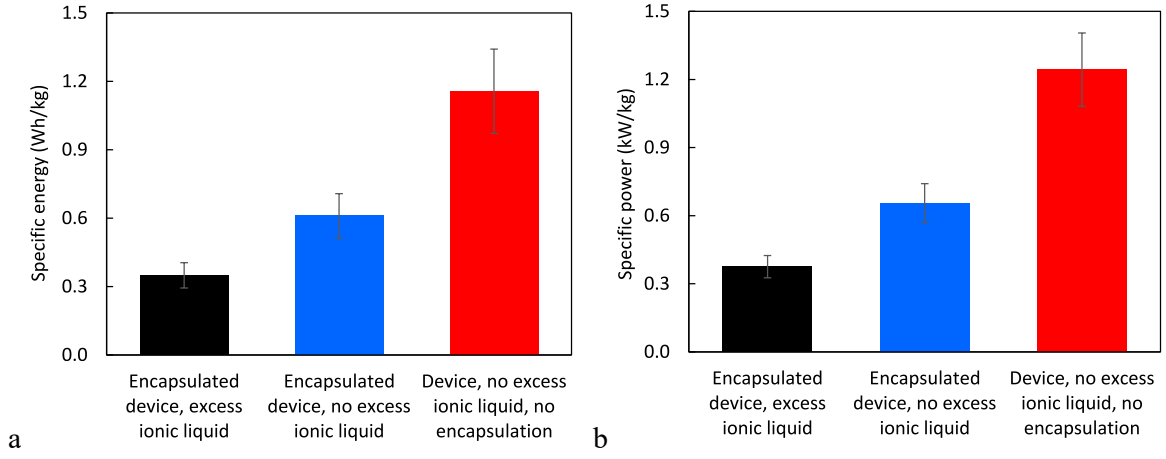

Fig. 11. (a) Specific energies and (b) maximum specific powers for various device mass configurations.

Fig. 13. Multifunctional fuselage beam demonstrator electrically connected to aircraft door model.

4. Conclusions

A demonstrator was fabricated to illustrate the concept of a multifunctional structural fuselage component that could power mechanical actuation of an aircraft passenger door in an emergency. Such a component could eliminate the mass and volume needed for conventional backup energy storage devices. This study investigated the effect of the applied pressure and quantified the inherent variability in the electrochemical characteristics between nominally-identical cells in a multicell structural supercapacitor composite component. A multifunctional C-section beam, representative of a fuselage component in a large airliner, was manufactured. The beam was 80 cm long × 20 cm wide × 10 cm deep and 7 mm thick in the web region and contained two stacks of four 30 cm × 15 cm × 0.5 mm structural supercapacitor cells within the web. These structural supercapacitors comprised of spread tow carbon fibre fabric electrodes reinforced with high surface area carbon aerogel to provide high capacitance and structural rigidity. A polymeric separator was bonded between the electrodes using patterned structural epoxy, and the whole laminate was infused with an ionic liquid electrolyte and encapsulated with protruding aluminium current collector tapes.

The multifunctional beam successfully opened and closed a desktop-scale aircraft door mechanism using three or four of the eight integrated cells connected in series after a short charge at 6 V. Greater applied pressure reduced the equivalent series resistance by enhancing the electrical contact between the current collector material and the carbon fibres reinforced with carbon aerogel. A loss of electrochemical performance was measured over time and after integration of the cells into the C-beam. A potential contributor to the loss in performance post-integration was considered to be ingress of moisture which could lead to parasitic water electrolysis.

Further work is required to develop improved solutions for lightweight and thinner (a) inert encapsulation with load transfer across all interfaces and (b) current collection, including efficient connections from the cells to the external electrical system(s). Further research also needs to develop solutions to (c) maintain through-thickness pressure after consolidation to achieve low contact resistances and (d) resolve issues with high self-discharge rates or parasitic reactions. Finally, to fully evaluate the multifunctional performance, mechanical characterisation of the structural power composite material and component is needed. Translation of structural power composite technology from the lab to larger scale components that are relevant to industry requires further research to address all of these technical hurdles. In particular, more studies should investigate scale-up issues and demonstration using multicell assemblies and complex geometry structural components. Solutions to these technical challenges would enable structural power composites to revolutionise future structural and electrical engineering applications.

Author statement

Sang Nguyen: Conceptualization, Methodology, Investigation, Data Curation, Formal Analysis, Validation, Visualization, Writing - Original Draft, Writing - Review & Editing. **David B Anthony:** Investigation, Methodology, Writing - Review & Editing. **Tomas Katafiasz**: Investigation, Visualization, Writing - Review & Editing. **Guocheng Qi**: Investigation, Methodology, Writing - Review & Editing. **Seyedalireza Razavi**: Investigation, Visualization. **Evgeny Senokos**: Methodology, Writing - Review & Editing. **Emile S Greenhalgh**: Conceptualization, Investigation, Methodology, Formal Analysis, Visualization, Writing - Review & Editing, Funding acquisition. **Milo S P Shaffer**: Formal Analysis, Writing - Review & Editing, Funding acquisition. **Anthony R J Kucernak**: Formal Analysis, Writing - Review & Editing, Funding acquisition. **Peter Linde**: Conceptualization, Writing - Review & Editing, Funding acquisition.

Declaration of competing interest

The authors declare that they have no known competing financial interests or personal relationships that could have appeared to influence the work reported in this paper.

Data availability

Data supporting this study are included within the article.

Acknowledgements

The authors acknowledge Jonathon Cole, Roland Hutchins, Gary Senior and Franco Giammaria for their advice and support with manufacturing of the demonstrator. This work was supported by the EPSRC Future Composites Research Manufacturing Hub (EP/P006701/1), the EPSRC Realising Structural Power project (EP/W035219/1), the European Office of Aerospace Research and Development (IOE Grant FA9550-17-1-0251), EU Clean Sky 2 (SORCERER Project #738085) and the Royal Academy of Engineering (Chair in Emerging Technologies). Data supporting this study are included within the article. For the purpose of open access, the author has applied a Creative Commons Attribution (CC BY) licence to any Author Accepted Manuscript version arising.

Appendix A. Supplementary data

Supplementary data to this article can be found online at https://doi.org/10.1016/j.compscitech.2023.110339.

References

[1] L.E. Asp, E.S. Greenhalgh, Chapter 20 - multifunctional structural battery and supercapacitor composites, in: K. Friedrich, U. Breuer (Eds.), Multifunct. Polym. Compos., William Andrew Publishing, Oxford, 2015, pp. 619–661, https://doi.org/10.1016/B978-0-323-26434-1.00020-9.

[2] D. Carlstedt, L.E. Asp, Performance analysis framework for structural battery composites in electric vehicles, Composites, Part B 186 (2020), 107822, https://doi.org/10.1016/j.compositesb.2020.107822.

[3] S.N. Nguyen, A. Millereux, A. Pouyat, E.S. Greenhalgh, M.S.P. Shaffer, A.R. J. Kucernak, et al., Conceptual multifunctional design, feasibility and requirements for structural power in aircraft cabins, J. Aircraft 58 (2021) 677–687, https://doi.org/10.2514/1.C036205.

[4] E. Karadotcheva, S.N. Nguyen, E.S. Greenhalgh, M.S.P. Shaffer, A.R.J. Kucernak, P. Linde, Structural power performance targets for future electric aircraft, Energies 14 (2021) 6006, https://doi.org/10.3390/en14196006.

[5] Y. Xu, W. Lu, G. Xu, T.-W. Chou, Structural supercapacitor composites: a review, Compos. Sci. Technol. 204 (2021), 108636, https://doi.org/10.1016/j.compscitech.2020.108636.

[6] F. Danzi, R.M. Salgado, J.E. Oliveira, A. Arteiro, P.P. Camanho, M.H. Braga, Structural batteries: a review, Molecules 26 (2021) 2203.

[7] J. Xu, Z. Geng, M. Johansen, D. Carlstedt, S. Duan, T. Thiringer, et al., A multicell structural battery composite laminate, EcoMat 4 (2022), e12180, https://doi.org/10.1002/eom2.12180.

[8] L.E. Asp, K. Bouton, D. Carlstedt, S. Duan, R. Harnden, W. Johannisson, et al., A structural battery and its multifunctional performance, Adv Energy Sustain Res 2 (2021), 2000093, https://doi.org/10.1002/aesr.202000093.

[9] E.S. Greenhalgh, L.E. Asp, STORAGE (Composite Structural Power Storage for Hybrid Vehicles) Final Summary Report, 2013. STORAGE/WP1/ICL/M1-42.

[10] J. Ankersen, M. Mistry, S. Nguyen, E.S. Greenhalgh, A. Kucernak, Addressing engineering issues for a composite structural power demonstrator, in: 19th Int. Conf. Compos. Mater., Montreal, Canada, 28 Jul - 2 Aug: ICCM19, 2013, pp. 1–10.

[11] M. Rana, Y. Ou, C. Meng, F. Sket, C. González, J.J. Vilatela, Damage-tolerant, laminated structural supercapacitor composites enabled by integration of carbon nanotube fibres, Multifunct Mater 3 (2020), 15001, https://doi.org/10.1088/2399-7532/ab686d.

[12] E.S. Greenhalgh, M.S.P. Shaffer, A.R. Kucernak, D.B.B. Anthony, E. Senokos, S. N. Nguyen, et al., Future challenges and industrial adoption strategies for structural supercapacitors, in: 22nd Int. Conf. Compos. Mater., Melbourne, Australia, 11-16 August: ICCM22, 2019, pp. 1–23.

[13] W. Johannisson, D. Carlstedt, A. Nasiri, C. Buggisch, P. Linde, D. Zenkert, et al., A screen-printing method for manufacturing of current collectors for structural batteries, Multifunct Mater 4 (2021), 35002, https://doi.org/10.1088/2399-7532/ac2046.

[14] G. Qi, S. Nguyen, D.B. Anthony, A.R.J. Kucernak, M.S.P. Shaffer, E.S. Greenhalgh, The influence of fabrication parameters on the electrochemical performance of multifunctional structural supercapacitors, Multifunct Mater 4 (2021), 34001, https://doi.org/10.1088/2399-7532/ac1ea6.

[15] F. Kruse, M. Kühn, C. Krombholz, H. Ucan, S. Torstrick, Production of a Full Scale Demonstrator-Structure within the FP7 Project Maaximus. 5th Int. Work. Aerostructures, German Aerospace Center, Manchester, GB, 2015, pp. 1–6.

[16] M. Moix-Bonet, D. Schmidt, P. Wierach, Structural health monitoring on the SARISTU full scale door surround structure, in: R. Lammering, U. Gabbert, M. Sinapius, T. Schuster, P. Wierach (Eds.), Lamb-Wave Based Struct. Heal. Monit. Polym. Compos., Springer International Publishing, Cham, 2017, pp. 463–475, https://doi.org/10.1007/978-3-319-49715-0_20.

[17] D.B. Anthony, E.S. Greenhalgh, T. Katafiasz, A.R.J. Kucernak, P. Linde, S. Nguyen, et al., Structural supercapacitor composite technology demonstrator, in: Proc. 20th Eur. Conf. Compos. Mater., Lausanne, Switzerland, 26-30 June: ECCM20, 2022, pp. 1–7.

[18] S. Nguyen, D.B. Anthony, H. Qian, C. Yue, A. Singh, A. Bismarck, et al., Mechanical and physical performance of carbon aerogel reinforced carbon fibre hierarchical composites, Compos. Sci. Technol. 182 (2019), 107720, https://doi.org/10.1016/j.compscitech.2019.107720.

[19] M.F. Pernice, G. Qi, E. Senokos, D.B. Anthony, S. Nguyen, M. Valkova, et al., Mechanical, electrochemical and multifunctional performance of a CFRP/carbon aerogel structural supercapacitor and its corresponding monofunctional equivalents, Multifunct Mater 5 (2022), 025002.

[20] Y. Wang, F.-K. Chang, Numerical and experimental evaluation of mechanical performance of the multifunctional energy storage composites, J. Compos. Mater. 56 (2021) 199–212, https://doi.org/10.1177/00219983211049504.

[21] H.C. Maxwell, Series Ultracapacitors Datasheet, BCAP0150 P270 T07, 2022. Document number 1013793.9.